Int. J. Electrochem. Sci., 15 **(2020)** 10759 – 10771, doi: 10.20964/2020.11.62

International Journal of ELECTROCHEMICAL SCIENCE
www.electrochemsci.org

Structural and Electrochemical Properties of $Li_{1.2}Ni_{0.16}Mn_{0.54}Co_{0.08}O_2$ - Al_2O_3 Composite Prepared by Atomic Layer Deposition as the Cathode Material for LIBs

Miaomiao Zhou[1], Jianjun Zhao[1], Shitao Qiu[1], Feng Tian[1], Oleksandr Potapenko [1,2], Shengwen Zhong[1,], Hanna Potapenko[1,2,*], Zhao Liang[1]*

[1] Faculty of Materials Metallurgy and Chemistry, Jiangxi University of Science and Technology, Ganzhou, Jiangxi, P.R. China
[2] Joint Department of Electrochemical Energy Systems, 38A Vernadsky Ave., Kiev 03142, Ukraine
[*]E-mail: zhongsw-jxust@outlook.com, avoloshka1982@gmail.com

Received: 28 July 2020 / *Accepted:* 16 September 2020 / *Published:* 30 September 2020

The atomic layer deposition (ALD) technique is used to coat Al_2O_3 on the lithium-rich cathode material $Li_{1.2}Ni_{0.16}Mn_{0.56}Co_{0.08}O_2$**.** Coating impacts on bulk and local structure changes are investigated by XRD method. SEM images indicate that the surface of the $Li_{1.2}Ni_{0.16}Mn_{0.56}Co_{0.08}O_2$ covered by Al_2O_3 has been protected from dissolution of cathode material and the modification of surface leads to formation of relatively rough layers of particles of $Li_{1.2}Ni_{0.16}Mn_{0.56}Co_{0.08}O_2$-$Al_2O_3$ composite. The initial capacity of coated $Li_{1.2}Ni_{0.16}Mn_{0.56}Co_{0.08}O_2$ cycled at 0.2C was 230 mAh·g-1 and a capacity retention of 93.6% was achieved after 100 cycles. Comparing the performance of uncoated Li-rich phase, there are significant improvements attributed to the Al_2O_3 ALD process without significantly affecting high rate applications. Thus, the ALD technique could be a feasible pathway for improved cycling for high capacity LIBs.

Keywords: lithium-rich cathode materials, co-precipitation, lithium-ion battery.

1. INTRODUCTION

Lithium ion batteries (LIBs) are integral part for different power the electronic portable devices that are ubitquitous in daily life owning to their high energy density and long cycle life[1, 2]. Cathode materials are one of the limiting factors in the capacity and longevity and necessitates continued research for new compositions or methods toward high capacities and energy densities[3, 4]. Currently, the lithium-rich layered cathode materials exhibit ultra-high specific capacity, often more than 250 $mAh \cdot g^{-1}$ and these unique capacities mark them as leading candidates for the next generation of LIBs [5, 6]. However, the lithium-rich layered cathodes still face issues such as low initial capacity and poor cycle life among others that seriously restrict their commercial application[7, 8, 9].

One of the most useful ways for improving the electrochemical properties of electrode material is surface modification. Common coating materials include simple oxides TiO_2[10], Al_2O_3[11], MgO_2[12], MnO_2[13], MoO_3[14] and CeO_2[15], phosphates $FePO_4$[16], $CoPO_4$ and $NiPO_4$, fluorides CaF_2, AlF_3 and SmF_3, organic polymers, lithium metal oxides $LiAlO_2$, Li_2ZrO_3, Li_2TiO_3, $Li_4Ti_5O_{12}$, Li_3VO_4 and $LiNiPO_4$ etc. The surface of $Li[Li_{0.17}Ni_{0.2}Co_{0.05}Mn_{0.58}]$, synthesized by a spray-drying method, was coated by CeO_2 at 1 wt%. These composite nanoparticles possessed an initial discharge capacity of 258.1 $mAh{\cdot}g^{-1}$ at 0.1C and after 80 cycles the capacity retention was 90.8%[17,18,19]. Zheng and Sun reported the deposition of an AlF_3 thin layer on Li-Mn based material improved multiple factors including reduced HF erosion from $LiPF_6$ breakdown and dissolution of electrode material, enhanced structural stability, and reduced voltage drops of the material during cycling[20, 21].

The surface modification of $Li_{1.2}Ni_{0.13}Co_{0.13}Mn_{0.54}O_2$ (NCM) by ZnO nanoparticles effectively reduced electrolyte decomposition that feeds deleterious side reactions at the surface of electrode materials [22]. NCM sample were also coated by 5 wt%. The initial discharge capacity was 230 $mAh{\cdot}g^{-1}$ at 0.2C and decreased to 215 $mAh{\cdot}g^{-1}$ (coulombic efficiency is 93.6%) after 100 cycles. At 1C the capacities were 185 $mAh{\cdot}g^{-1}$ and maintained 165 $mAh{\cdot}g^{-1}$ after 100 cycles (coulombic efficiency was 86.3%)[23]. An Al_2O_3 layer (reported as ~ 6 nm) was deposited on $LiNi_{0.7}Co_{0.15}Mn_{0.15}O_2$. The initial discharge capacity was 175 $mAh{\cdot}g^{-1}$ and decreased to 125 $mAh{\cdot}g^{-1}$ at 0.5C after 130 cycles (coulombic efficiency was 90%) [24].

The composition Li1.2Ni0.13Co0.13Mn0.54O2 with Al_2O_3 coating gave an initial discharge capacity of 317.9 mAh·g-1 at the low 0.1C rate but maintained 164 mAh·g-1 at 2C after 200 cycles (coulombic efficiency is 86.3%) [25].

Given the wealth of approaches toward coating we have prepared a Li-rich layered $Li_{1.2}Ni_{0.16}Mn_{0.56}Co_{0.08}O_2$ oxide and then modified with Al_2O_3 nanoparticles via atomic layer deposition. The electrochemical performance, surface morphology, and thermal stability are investigated to evaluate the effect of the surface modification with Al_2O_3 nanoparticles. It is demonstrated that the electrochemical properties of the $Li_{1.2}Ni_{0.16}Mn_{0.56}Co_{0.08}O_2$ oxide are improved by the surface modification and this coated material achieves competitive performance with other materials for the next generation of lithium-ion battery technologies.

2. EXPERIMENTAL SECTION

2.1. Synthesis of materials

$MnSO_4{\cdot}H_2O$, $NiSO_4{\cdot}6H_2O$ and $CoSO_4{\cdot}7H_2O$ (Sigma Aldrich, 99%) salts were mixed in stoichiometric ratios of 0.54:0.16:0.08 and dissolved 1.0 L of deionized water with stirring to give a total metal ion concentration of 2 mol/L. A mixture of NaOH (4 M) and NH_4OH were mixed to make a alkaline feed mixture with a pH ~ 11.0. The feed rate of the salt solution and alkaline solutions were controlled by the slow rate titrate stainless steel tank reactor constantly under N_2 flow. The pH value was maintained at 11.0 ± 0.05 and the reactor temperature was held at 55°C. The black powder of the $Ni_{0.2}Mn_{0.7}Co_{0.1}(OH)_2$ precursor was obtained by vacuum filtration and dried at 100°C for 24 h. Finally,

the target compounds were obtained by the heat treatment of the precursor mix with $LiOH{\cdot}4H_2O$ at 900°C for 12 h in air.

The atomic layer deposition is a method for growing uniform ultrathin layers that are obtained at the relatively low precipitation temperature that it is easy to operate with the precipitates. The aluminum and oxygen nanoparticles content are deposited from C_3H_9Al (TMA) and distilled water is used as the solvent.

2.2. Characterizations

Crystal phase analysis of Li1.2Ni0.16Mn0.56Co0.08O2 and Al2O3-NCM materials were examined by X-ray diffraction (XRD), using a MiniFlex 600 (Rigaku, Japan) with Cu Kα wavelength (voltage and current settings) Morphology was assessed by transmission electron microscopy (JEM-2100, JEOL, Tokyo, Japan) and scanning electron microscopy on a (JSM-7800F, Tokio, Japan), with an acceleration voltage at 15 - 20 kV in back scatter (SE) detection mode.

2.3. Electrochemical Measurements

Cathode active materials were mixed in a weight ratio of 8:1:1, with Super P and PVDF and then N-methyl-2-pyrrolidone (NMP) was added for agate ball milling to produce a slurry. The slurry was coated on Al foil and vacuum dried for 12 h at 80 °C. The electrolyte was 1 M $LiPF_6$ in 1:1 v/v ethylene carbonate (EC) and dimethyl carbonate (DMC). Once dried, electrodes were cut into circular pieces, use, Lithium metal is used as symmetrical electrode, These cathodes were assembled into two-electrode CR2032-type coin cells with dried NCM/-coated cathodes, Celgard separator 2500, and Lithium metal counter electrode. The test cells were assembled in a glove box filled with high-purity argon and trace water and O_2 levels.

The measured loading of active material was 2.5~3.5 mg in the cathode with a diameter of 12 mm and a thickness of ~ 60 mm for all electrode materials. The electrolyte volume used during the coin cell assembly was ~500 μL. Galvanostatic cycling tests were performed at different current densities in a voltage range of 2.7 - 4.6 V vs. Li^+/Li metal using a LAND testing system (Jinnuo, Wuhan, China). The current density corresponding to 1 C was 274 $mA{\cdot}g^{-1}$

3. RESULT AND DISCUSSION

3.1. Structural features

The XRD patterns for bare (NCM) and ALD-coated (Al_2O_3-NCM) positive electrode materials are shown in Fig. 1(a). The diffraction peaks corresponded to all reflections are specific for α-$NafeO_2$ layered structures, which belongs to *R-3m* space group. Moreover, two pairs of signals ((006)/(102) and (108)/(110)) are obviously divided, which conforms to the typical characteristics of layered structure,

indicating the high orderliness of simples and the two-dimensional layered structure are formed. In addition, the group of small diffraction peaks, which demonstrate the presence of monoclinic Li_2MnO_3 phase appeared between 2θ =20°-25°. It has been observed that the diffraction peaks of materials have not changed significantly before and after cycling, indicating the high stability and purity of synthesized samples. **In Fig.1(b)** the absence of changing a structure after 100 cycles at the 1C discharge current rate is shown, indicating a stabile state of diffraction peaks for two materials still have the α-$NafeO_2$ structure. It is shown that the reflections are shifted to the lower angles for both materials after 100 cycles, that indicate the increasing a lattice parameters for the samples upon cycling. There are shifts to the lower angles for both materials after 100 cycles, most likely lattice expansion from the insertion/removal of lithium during cycling. The migration of (003) peak for Al_2O_3-NCM is smaller than for pristine NCM. This suggests that ALD coating may inhibit the structural expansions resulting from electrochemical tests and improves the structural stability of the lithium-manganese based positive electrode material [26, 27].

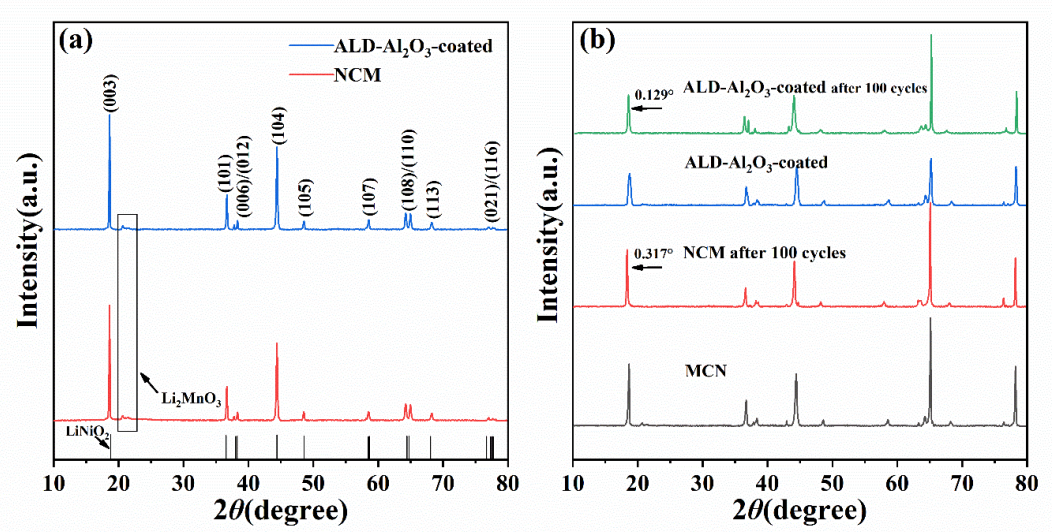

Figure 1. XRD patterns of (a) the pristine and Al_2O_3-NCM samples; (b) NCM and Al_2O_3-NCM materials incorporated in cathode electrodes initially and after 100 cycles.

Table 1. Structure parameters of the pristine and Al_2O_3-NCM materials.

Samples	a(Å)	c(Å)	c/a	I_{003}/I_{104}
NCM	2.8684	14.2732	4.9760	1.6864
Al_2O_3-NCM	2.8679	14.2718	4.9764	1.5929

The *c/a* parameters for both materials are shown in **Table 1.** These values are in close agreement and larger than 4.9. The I(003)/I(104) ratios are both much higher than 1.2 and this ratio is an indication of ordered cation distribution. The cation disorder and possible Li ion disorder for the Al_2O_3-NCM

sample is higher and may be a consequence of the ALD process near the surface. After coating the c/a ratio slightly increases, which leads to improving an electrochemical performance of coating material.

3.2. SEM and TEM analysis

In **Figure 2** the SEM micrographs of NCM and Al_2O_3-NCM materials is ` It is shown that all samples consist of spherical particles with primary average size of 0.5-1.5μm and secondary particle size is 5-10μm (Fig.2 (a, b, c, d)). It is known that during the electrochemical process, the reactive area for primary particles can increase and the diffusion path of lithium ions is greatly short, which would be a significant factor affecting an electrochemical performance of electrode materials [28, 29]. As follows from microphotographs, the surfaces of the samples are coated become a little rough in comparison with a bare is relatively smooth covering. The TEM images are shown in **Fig.2 (e)** which demonstrates the extra coated layer can be clearly observed on the particle more clearly. Thus, the presence of extra layer can reduce the contact area between the material and electrolyte, the occurrence of side reactions are slowed down or inhibited, and the rate performance of the material is more stable [30, 31].

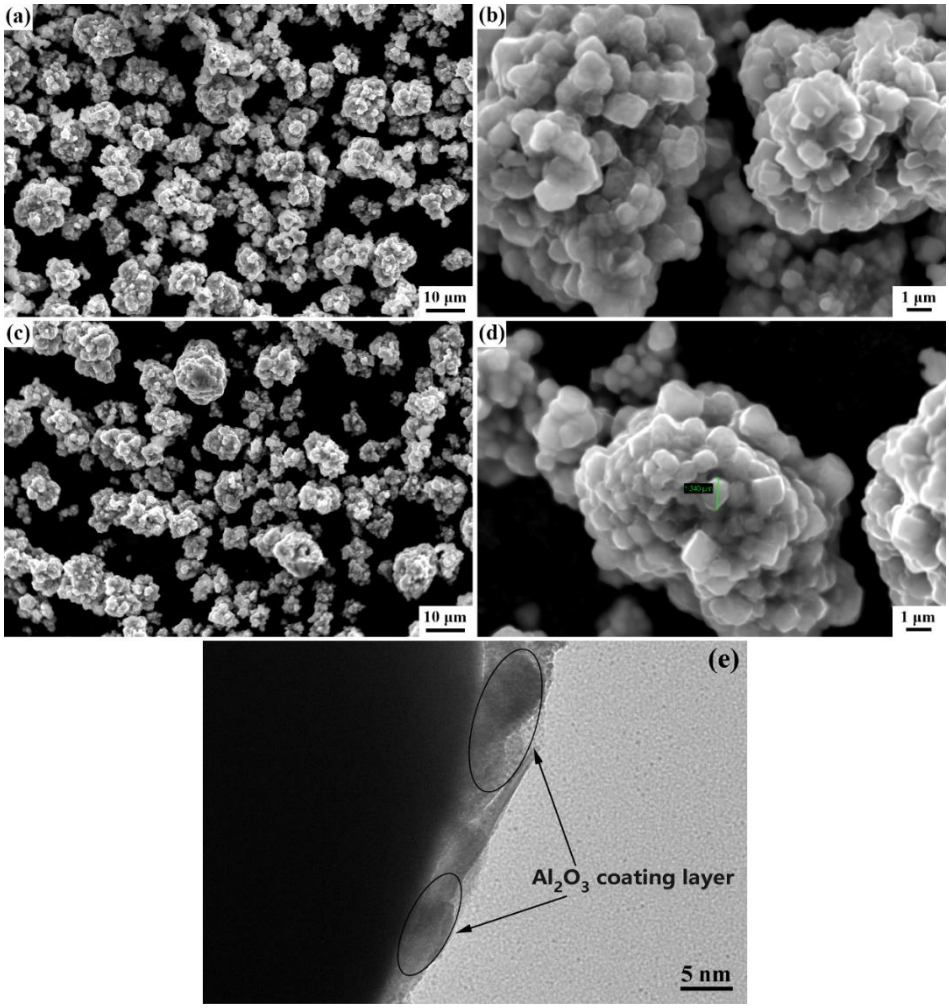

Figure 2. SEM images for NCM (a),(b) and Al_2O_3-NCM (c), (d); TEM image displaying the coating layer of Al_2O_3 for Al_2O_3-NCM materials (e).

The agglomerated particles before electrochemical testing are spherical as it is shown **in Fig.3 (a, b)**. **In Fig.3 (c, d)** the microphotographs of the positive electrode after 100 cycles at current density 1C are shown. It is observed that the uncoated material is broken to a certain extent and becomes dispersed without agglomeration (Fig. 3 (d)). Upon cycling for 100 cycles, the spherical particles remain intact, except that the surface of them became a little rough, as is shown in Fig. 3 (c).

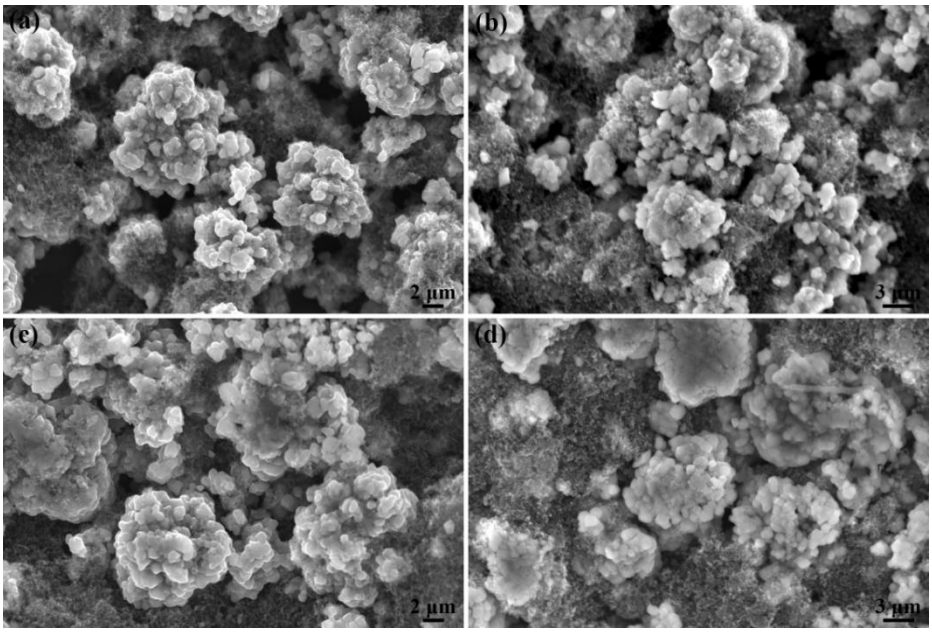

Figure 3.(a) SEM images of the pristine Al_2O_3-NCM material (a, b) and the micrographs of the Al_2O_3-NCM samples after 100 cycles (c, d).

3.3 Electrochemical properties

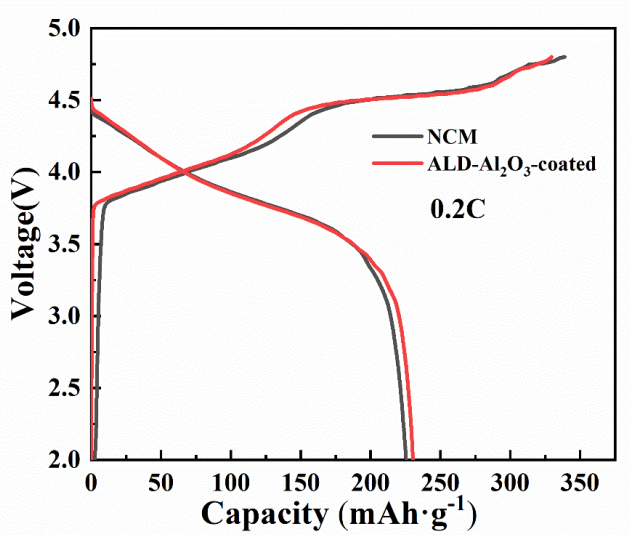

Figure 4. The first charge-discharge curves of the NCM and Al_2O_3-NCM materials at 0.2C in the range of potentials 2.0 - 4.8 V.

The initial charge-discharge profiles of NCM and Al_2O_3-NCM material in the range of 2.0 – 4.8 V at 0.2C are shown in **Figure 4** and **Table 2**. The first plateau (< 4.5 V) is the oxidation process of $Ni^{2+} \rightarrow Ni^{4+}$ and $Co^{3+} \rightarrow Co^{4+}$, and the 2nd plateau is the further extraction of Li and O from the irreversible activation of Li_2MnO_3 at ~4.5 V [32] The 1st full cycle of the materials shows no significant structural change and was supported by the XRD results.

Table 2. The first charge/discharge capacities are collected at 0.2C in the range of 2.0 - 4.8 V for the NCM and Al_2O_3-NCM materials.

Samples	Charge capacity ($mA \cdot g^{-1}$)	Discharge capacity ($mAh \cdot g^{-1}$)	Irreversible capacity loss ($mAh \cdot g^{-1}$)	Coulomb efficiency (%)
NCM	354	225	129	63.6
Al_2O_3-NCM	330	230	100	69.7

Figure 5 displays the discharge curves of NCM and Al_2O_3-NCM samples after 100 cycles at different current loads between 2.0 – 4.6 V. The specific capacity for NCM material is changed from 172.6 $mAh \cdot g^{-1}$ to 152.1 $mAh \cdot g^{-1}$, and the capacity retention is 88.1% for this electrode at 0.2C upon 100 cycles. Thereafter, when the current density is elevated to 1C for the NCM sample, the specific discharge capacity is reduced from 172.7 $mAh \cdot g^{-1}$to 87.1 $mAh \cdot g^{-1}$, respectively, and the capacity retention is only 50.4%.

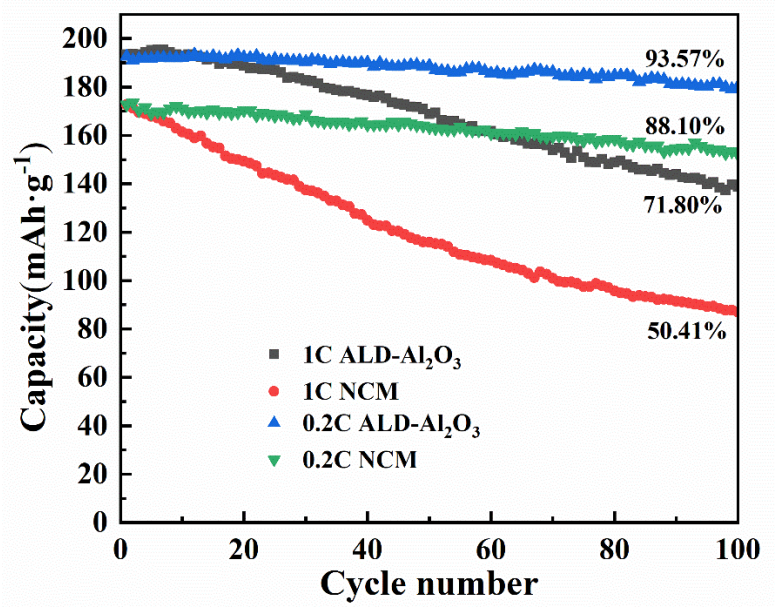

Figure 5. Discharge capacity of the NCM and Al_2O_3-NCM materials at 0.2C and 1C in the potential range of 2.0 – 4.6 V for 100 cycles.

Unlike this sample, the Al_2O_3-NCM material demonstrates higher coulomb efficiency 93.6% at 0.2C, and 71.8% at 1C, accordingly. These improvements are attributed to the high purity and conformal nature of Al_2O_3 grown by ALD that protects the material surface and provides better cycling over time for the materials [33].

Table 3. Comparison of reported electrochemical results of surface-coated electrode materials.

Samples	Coating material	Voltage range (V)	Current density ($mA \cdot g^{-1}$)	Initial capacity ($mAh \cdot g^{-1}$)	Number of cycles	Capacity after cycling ($mAh \cdot g^{-1}$)	Capacity retention (%)	Ref.
$Li_{1.2}Mn_{0.54}Ni_{0.13}Co_{0.13}O_2$	Y_2O_3	2.0-4.8	125	280	200	-	89	[34]
$Li_{1.2}Ni_{0.2}Mn_{0.6}O_2$	LiF	2.0-4.8	20	260	60	-	89	[35]
$Li_{1.2}Mn_{0.567}Ni_{0.167}Co_{0.066}O_2$	MnO_2	2.0-4.6	100	299	50	-	93	[36]
$Li_{1.2}Mn_{0.54}Ni_{0.13}Co_{0.13}O_2$	Polyanil-ine	2.0-4.8	50	238	200	189	79	[37]
$Li_{1.2}Mn_{0.54}Ni_{0.13}Co_{0.13}O_2$	Li_3PO_4	2.0-4.8	40	226	100	-	78	[38]
$Li_{1.2}Ni_{0.3}Mn_{0.57}O_2$	Li_2TiO_3	2.0-4.8	100	-	100	105	87	[39]
$Li_{1.8}Mn_{0.7}Ni_{0.15}Co_{0.15}O_{2.675}$	Li_2SiO_3	2.5-4.8	-	-	200	150	94	[40]
$Li_{1.2}Mn_{0.54}Ni_{0.16}Co_{0.08}O_2$	Al_2O_3	2.0-4.6	137	195	100	182	94	This work
$Li_{1.2}Mn_{0.54}Ni_{0.16}Co_{0.08}O_2$	Al_2O_3	2.0-4.6	274	173	100	152	88	This work

The values collated in **Table 3** are comparable to our AL_2O_3-NCM material. The critical parameters for electrode materials are specific capacities after power tests and capacity retention upon extended cycling. Our $Li_{1.2}Mn_{0.54}Ni_{0.16}Co_{0.08}O_2$ - Al_2O_3 coated material has the highest capacity retention (94%) among similar compositions[34, 35, 37, 38, 39] and the specific capacity is near the best materials [40] upon cycling. These comparisons again point to the improved performance using an ALD method to apply the Al_2O_3 layer to the active material.

The discharge capacities on 3-rd, 20-th, 50-th, 80-th and 100-th cycles for both samples are presented in Fig. 6 (a, b). The discharge curves for the electrodes are shifted to the low-voltage region differently[41]. However, in comparison with the uncoated material, the discharge vo]ltage plateauforAl_2O_3-NCM sample drops more slowly and moves less. It is clearly observed from Fig.6 (b, c), the initial discharge profile for the pristine electrode shows a significant downward trend, while the electrode almost is not changed. The discharge curves for the uncoated and the coated electrodes after

the third and–100-th cycles are shown in Fig. 6 (e, f). In comparison with the NCM electrode, the polarization between charge and discharge after 100 cycles for the Al_2O_3-NCM electrodes is much smaller. This small polarization effect for Al_2O_3-NCM garners better reversibility of the electrochemical process. Some polarization stems from the side reactions from electrolyte breakdown which can also be ameliorated with the Al_2O_3 coating[42]. Thus, the guarantee the stability of layered structures, the specific capacity and cycle stability can be improved, and adverse reactions on the electrode surface can be reduced for positive electrode materials with a layer structure.

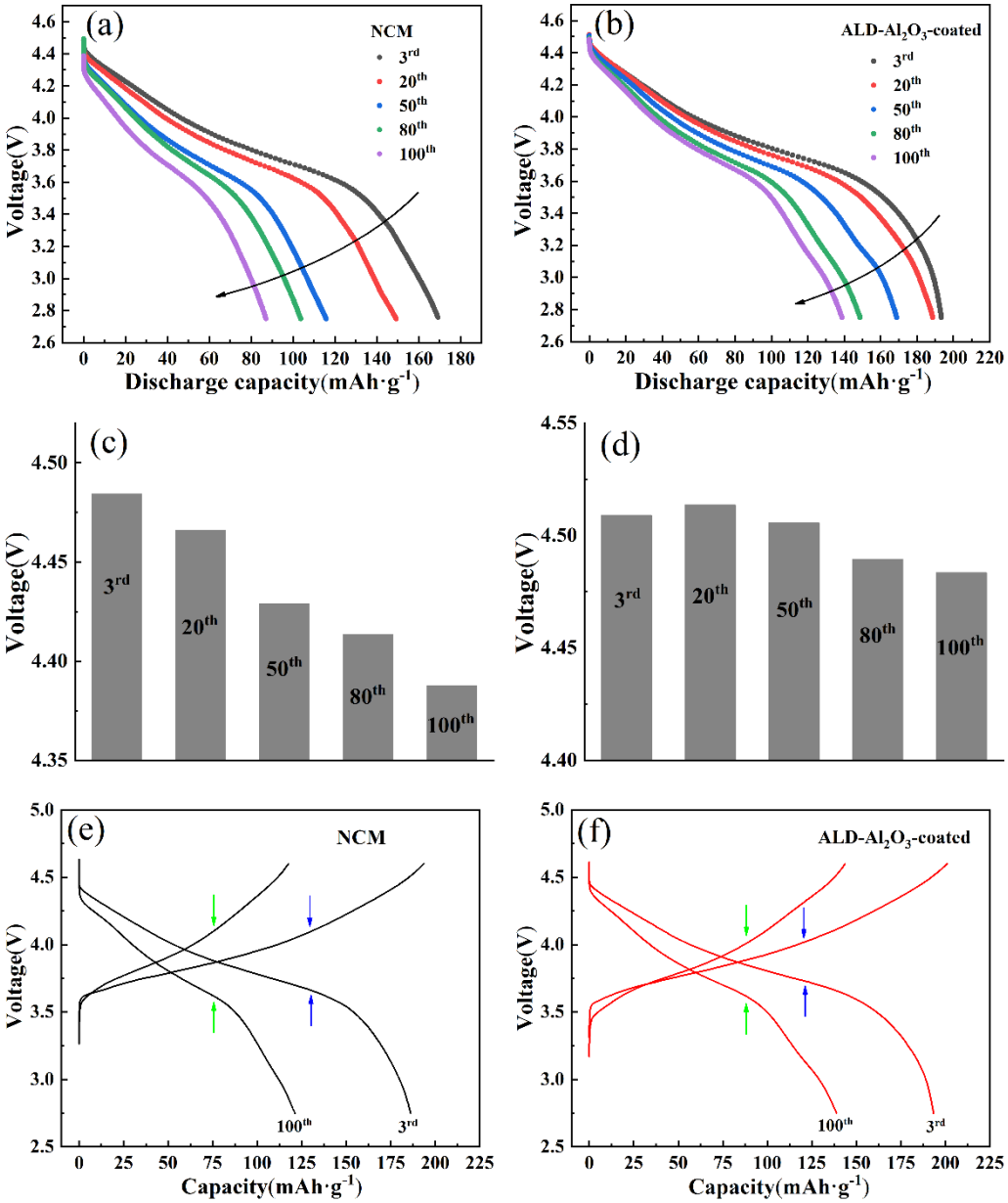

Figure 6. The galvanostatic charge/discharge profiles for the (a) NCM and (b) Al_2O_3-NCM materials; voltage drop on 3rd, 20th, 50th, 80th and 100th cycles for both materials (c), (d); the charge/discharge curves for the (e) NCM and (f) Al_2O_3-NCM materials for the 3^{rd} and 100^{th} cycles.

The discharge rate capacity retention was tested for both samples from 0.1C to 2C for 5 cycles. These results are shown in **Fig. 7.** It can be seen that with the increasing current density, the discharge capacity of the pristine sample decreases rapidly. The Al_2O_3-NCM electrode returns to 150 $mAh \cdot g^{-1}$ at 2C. After ramping the current density and returning to the initial rate of 0.1C, the specific discharge capacity of Al_2O_3-NCM and NCM were 196 and 170.3 $mAh \cdot g^{-1}$, respectively. These correspond to capacity retentions of 99.4 % and 96.8 % after 25 cycles. The ultrathin surface modification with Al_2O_3 dramatically increased the high rate capacity by a factor of nearly 10x comparing 0.2 C for NCM and 2 C for Al_2O_3-NCM.

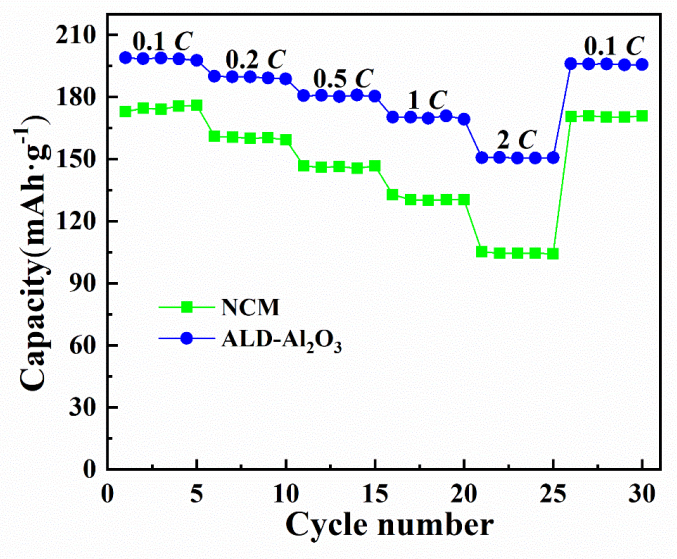

Figure 7. The rate performance of the NCM and Al_2O_3-NCM materials in the range of potentials 2.0 - 4.6 V.

Figure 8 shows the cyclic voltammetry (CV) data in the potential range of 2.0 – 4.6 V at a scan rate of 0.1 mVs-1. The NCM electrode has two strong oxidation peaks at 4.2 V and 4.6 V (**Fig. 4(a)).** The maximum at 4.2 V represents the oxidation process of $Ni^{2+} \rightarrow Ni^{4+}$ and $Co^{3+} \rightarrow Co^{4+}$ [43]. The peak at 4.6 V is caused by the activation stage of Li_2MnO_3. Moreover, the absence of new redox peak in the CV curve for the coated material is seen, and the coating does not participate in the charge/discharge reactions [44]. In comparing with the pristine sample, the oxidation peak of Al_2O_3 at 4.6V is reduced (**Fig. 8b**), and the irreversibility of this process is weakened. Thus, coating technique can inhibit the oxidation of the electrolyte and improve the coulomb efficiency and cycling performance of the material. After activation of Li_2MnO_3, the reduction of Mn^{4+} ions in MnO_2, is occurred at ~ 3.3V, and a weak oxidation peak is observed in the NCM electrode for $Mn^{3+} \rightarrow Mn^{4+}$.

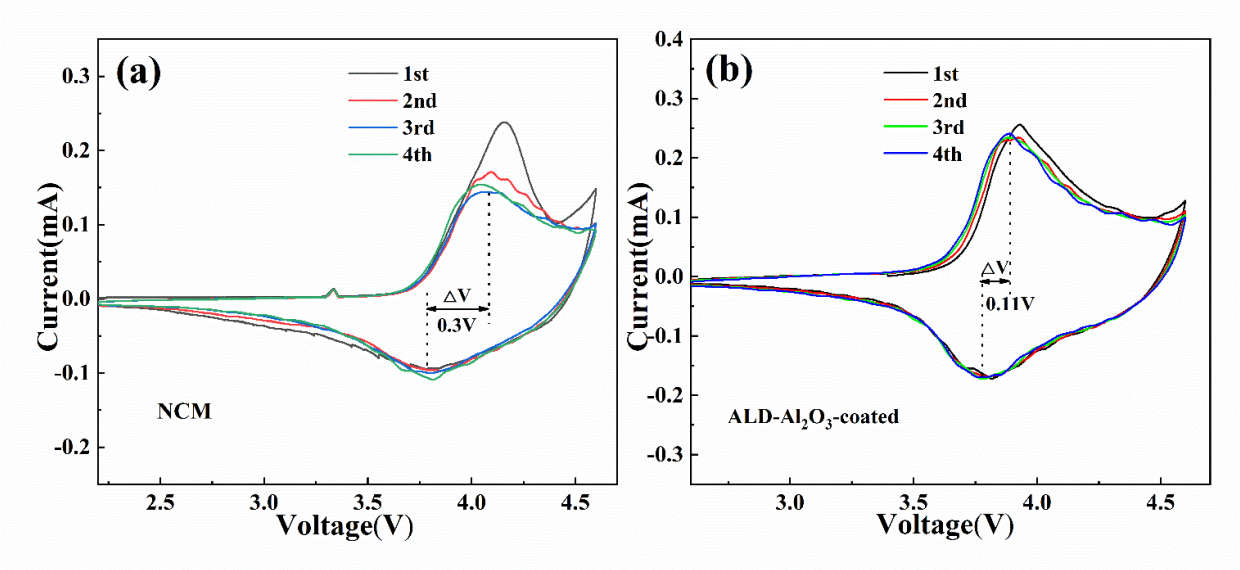

Figure 8. Cyclic voltammograms at a scan rate of 0.1 mVs^{-1} between 2.0 V- 4.8 V of the (a) NCM and (b) Al_2O_3-NCM materials.

4. CONCLUSION

The ALD technique was used to obtain a $Li_{1.2}Ni_{0.16}Mn_{0.56}Co_{0.08}O_2$- Al_2O_3 coated porous powder. The Al_2O_3-NCM material has a typical layered structure with the well-studied Li_2MnO_3 activation layer. Electrochemical tests show that the Al_2O_3-NCM sample has a capacity retention of 93.57% after 100 cycles at 0.2C, which outperformed the NCM electrode (88.1%). Furthermore, it is suggested that the coating layer helps mitigate deleterious electrolyte side reaction with the surface of the material. The surface modification layer of Al_2O_3 using atomic layer deposition is an effective way to improve the electrochemical performance for $Li_{1.2}Ni_{0.16}Mn_{0.56}Co_{0.08}O_2$. This approach should be considered for other candidate cathode materials as research continues to meet the battery power and longevity demands of the future.

ACKNOWLEDGMENTS
This work was supported by the National Natural Science Foundation of China (51874151),the Scientific Research Foundation for universities from the Education Bureau of Jiangxi Province(GJJ170510), the Natural Science Foundation of Jiangxi Province(20151BBE50106) and the Jiangxi University of Science and Technology (NSFJ2014-G13, Jxxjbs12005).

References

1. J.B. Goodenough, Y. Kim, *Chem. Mater.*, 22 (2010) 587.
2. J.T. Han, H.F. Zheng, Z.Y. Hu, X. R. Luo, Y.T. Ma, Q.S. Xie, D.L. Peng, G.H. Yue, *Electrochim. Ac ta,* 299 (2019) 844.
3. H.H. Zheng, J. Li, X.Y. Song, G. Liu, V.S. Battagliab, *Electrochim. Acta*, 71 (2012) 258.

4. X.Q. Yu, Y.C. Lyu, G. Lin, H.M. Wu, S.M. Bak, Y.N. Zhou, K. Amine, S.N. Enrlich, H. Li, K.W. N am, X. Q. Yang, *Adv. Energy Mater.,* 4 (2014) 1300950.
5. T.L. Zhao, L. Li, R.J Chen, H.M. Wu, X.X. Zhang, S. Chen, M. Xie, F. Wu, J. Lu, K. Amine, *Nano Energy*, 15 (2015) 164.
6. J. Lin, D.B. Mu, Y. Jin, B.R. Wu, Y.F. Ma, F. Wu, *J. Power Sources*, 230 (2013) 76.
7. Z.J. He, Z.X. Wang, H. Chen, Z.M. Huang, X.H. Li, H.J. Guo, R.H. Wang, *J. Power Sources,* 299 (2 015) 334.
8. P.H. Xiao, Z.Q. Deng, A. Manthiram, G. Henkelman, *J. Phys. Chem. C*., 116 (2012) 23201.
9. Y.P. Deng, F. Fu, Z.G. Wu, Z.W. Yin, T. Zhang, J.T. Li, L. Huang, S.G. Sun, *J. Mater. Chem. A.,* 4 (2 016) 257.
10. L.H. Yu, X.P. Qiu, J.Y. Xi, W.T. Zhu, L.Q. Chen, *Electrochim. Acta*, 51 (2006) 6406.
11. Y.Y. Huang, J.T Chen, F.Q Cheng,W. Wan,W. Liu, H.H.Zhou, X.X. Zhang, *J. Power Sources*, 195 (2010) 8267.
12. E. Han, Y.P. Li, L.Z. Zhu, L.Zhao, *Solid State Ionics*, 255 (2014) 113.
13. G. Liu, C.X. Kang, J. Fang, L.K. Fu, H.H. Zhou, Q.M. Liu, *J. Power Sources,* 431 (2019) 48.
14. J. Huang, X. Fang, Y. Wu, L. Zhou, Y. Wang, Y. Jin, W. Dang, L.P. Wu, Z.H. Rong, X. Chen, X.C. T ang, *J. Electroanal. Chem*., 823 (2018) 359.
15. F. Wu, M. Wang, Y.F. Su, L.Y. Bao, S. Chen, *Electrochim. Acta,* 54 (2009) 6803.
16. Z.Y. Wang, E.Z. Liu, C.N. He, C.S. Shi, J.J. Li, N.Q. Zhao*, J. Power Sources,* 236 (2013) 25.
17. W. Yuan, H.Z. Zhang, Q. Liu, G.R. Li, X.P. Gao, *Electrochim. Acta,* 135 (2014) 199.
18. P.Y. Guan, L. Zhou, Z.L. Yu, Y.D. Sun, Y.J. Liu, F.X. Wu, Y.F. Jiang, D.W. Chu, *J Energy Chem*., 43 (2020) 220.
19. B.T. Zhao, R. Ran, M.L. Liu, Z.P. Shao, *Mater. Sci. Eng., R.* 98 (2015) 1.
20. J.M. Zheng, M. Gu, J. Xiao, B.J. Polzin, P.F. Yan, X.L. Chen, C.M. Wang, J.G. Zhang, *Chem. Mate r.,* 26 (2014) 6320.
21. Y.K. Sun, M.J. Lee, C.S. Yoon, J. Hassoun, K. Amine, B. Scrosati, *Adv. Mater.*, 24 (2012) 1276.
22. R.B. Yu, Y.B. Lin, Z.G. Huang, *Electrochim. Acta*, 173 (2015) 515.
23. A. Martens, C. Bolli, A. Hoffmann, C. Erk, T. Ludwig, K.M. EI, U. Breddemann, P. Novák, I. Kros sing, *J. Electrochem. Soc.,* 167 (2020) 070510.
24. H. Jung, W. Park, J. Holder, Y.J. Yun, S. Bong, *J. Nanosci. Nanotechnol.,* 20 (2020) 6505.
25. T. Zou, W.J. Qi, X.S. Liu, X.Q Wu, D.H. Fan, S.H. Guo, L. Wang, *J. Electroanal. Chem.,* 859 (202 0) 113845.
26. X.F. Zhang, I. Belharouak, L. Li, Y, Lei, J.W. Elam, A. Nie， X.Q. Chen， R.S. Yassar, R.L, Alelba um, *Adv. Energy Mater*., 3 (2013) 1299.
27. K.H, Anulekha, A.N. Quan, F.S. Botao, B.Rachel, L.B. Sibani, *ACS Appl. Energy Mater.,* 3 (2019) 4 56.
28. N. Anton, A. Ali, A. Michel, G. Torbjörn, O.T. John, *Electrochem. Commun.*, 7 (2005) 156.
29. Z. Wang, Y.P. Yin, Z.Y. Wang, M. Gao, T.Y. Ma, W.D. Zhuang, S.G. Lu, A.L. Fan, K. Amine, Z.H. Chen, *Nano Energy*, 31 (2017) 247.
30. G.S. Zou, X.K. Yang, X.Y. Wang, L. Ge, H.B. Shu, Y.S. Bai, C. Wu, H.P. Guo, L. Hu, X. Yi, J. Bowei, H. Hu, D. Wang, R.Z. Yu, *J. Solid State Electrochem*., 18 (2014) 1789.
31. P.F. Yan, J.M. Zheng, X.F. Zhang, R. Xu, K.Amine, J. Xiao, J.G. Zhang, C.M. Wang, *Chem. Mater.,* 28 (2016) 857.
32. J. Rana, J.K. Papp, Z. Lebens-Higgins, M. Zuba, L.A.Kaufman, A. Goel, R. Schmuch, M. Winter,M. S. Whittingham, W. Yang, B.D. McCloskey, L.F.J.Piper, *ACS Energy Lett.,* 5 (2020) 634.
33. Y.K. Zhou, P.F. Bai, H.Q. Tang, J.T. Zhu, Z.Y. Tang, *J. Electroanal. Chem.,* 782 (2016) 256.
34. Q.C. Chen, L.M. Luo, L. Wang, T.F. Xie, S.C. Dai, Y.T. Yang, Y.P. Li, M.L. Yuan, *J. Alloys Compd.,* 735 (2018) 1778.
35. T.L. Zhao, L. Li, R.J. Chen, H.M. Wu, X.X. Zhang, S.Chen, M. Xie, F. Wu, J. Lu, K. Amine, *Nano Energy*, 15 (2015) 164.

36. S.H. Guo, H.J. Yu, P. Liu, X.Z. Liu, D. Li, M.W. Chen, H.S. Zhou, *J. Mater. Chem. A.,* 2.12 (2014) 4422.
37. X.W. Lai, G.R. Hu, Z.D. Peng, H.Tong, Y.Z. Wang, X.Y. Qi, Z.C. Xue, Y. Huang, K. Du, Y. B. Cao, *J. Power Sources*, 431 (2019) 144.
38. D.R. Chen, F. Zheng, L.Li, M. Chen, X.X. Zhong, W.S. Li, L. Lu, *J. Power Sources,* 341 (2017) 14 7.
39. E.Y. Zhao, X.F. Liu, Z.B. Hu, L.M. Sun, X.L. Xiao, *J. Power Sources,* 294 (2015) 141.
40. K. Gao, S.X. Zhao, S.T. Guo, C.W. Nan, *Electrochim. Acta,* 206 (2016) 1.
41. X.H. Liang, H.J. Wu, H.Y. Chen, *Int. J. Electrochem. Sci.,* 11 (2016) 9164.
42. J.P. Wang, C.Y. Du, C.Q. Yan, X.S. He, B. Song, G.P. Yin, P.J. Zuo, X.Q. Cheng, *Electrochim. Acta,* 174 (2015) 1185.
43. M. Iftekhar, N.E. Drewett. A.R. Armstrong, D. Hesp, F. Braga, S. Ahmed, L.J. Hardwick, *J. Electro chem. Soc.,* 161 (2014) A2109.
44. H.D Liu, D.N. Qian, M.G. Verde, M.H. Zhang, L. Baggetto, K.An, Y. Chen, K.J. Carroll.D. Lau, M. F. Chi, G. M. Veith, Y.S. Meng, *ACS appl. Mater. Interfaces,* 7 (2015) 19189.